Biochemical and Biophysical Research Communications 371 (2008) 33–38

Contents lists available at ScienceDirect

Biochemical and Biophysical Research Communications

journal homepage: www.elsevier.com/locate/ybbrc

Essential roles of caspases and their upstream regulators in rotenone-induced apoptosis

Jihjong Lee [a], Ming-Shyan Huang [b], I-Chi Yang [c], Tsung-Ching Lai [d], Jui-Ling Wang [d], Victor Fei Pang [a], Michael Hsiao [d,*], Mark Y.P. Kuo [c,e,*]

[a] Graduate Institute of Veterinary Medicine, College of Biological Resources and Agriculture, National Taiwan University, Taipei, Taiwan
[b] Department of Internal Medicine, Kaohsiung Medical University, Kaohsiung, Taiwan
[c] Graduate Institute of Oral Biology, College of Medicine, National Taiwan University, Taipei, Taiwan
[d] Genomics Research Center, Academia Sinica, Taipei, Taiwan
[e] Department of Dentistry, National Taiwan University Hospital, National Taiwan University, Taipei, Taiwan

ARTICLE INFO

Article history:
Received 14 March 2008
Available online 8 April 2008

Keywords:
Rotenone
Oral cancer
Apoptosis
Caspase activation

ABSTRACT

In the present study, we examined whether caspases and their upstream regulators are involved in rotenone-induced cytotoxicity. Rotenone significantly inhibited the proliferation of oral cancer cell lines in a dose-dependent manner compared to normal oral mucosal fibroblasts. Flow cytometric analysis of DNA content showed that rotenone treatment induced apoptosis following G2/M arrest. Western blotting showed activation of both the caspase-8 and caspase-9 pathways, which differed from previous studies conducted in other cell types. Furthermore, p53 protein and its downstream pro-apoptotic target, Bax, were induced in SAS cells after treatment with rotenone. Rotenone-induced apoptosis was inhibited by antioxidants (glutathione, *N*-acetylcysteine, and tiron). In conclusion, our results demonstrate significant involvement of caspases and their upstream regulators in rotenone-induced cytotoxicity.

Rotenone is a naturally occurring plant compound derived from the root and bark of some *Luguminosae* species (*Derris. Tephrosia* and *Lonchocharpus*). This compound is a specific inhibitor of mitochondrial complex I, and is the main ingredient in many botanical insecticides that have been used for at least 150 years to control vegetable pests. Administration of rotenone has been shown to lead to biochemical, anatomical, and behavioral symptoms resembling Parkinson's disease due to neurotoxicity [1–3]. Previous studies have shown that inhibiting mitochondrial complex I leads to cytochrome *c* release, followed by DNA fragmentation and cell death [4]. Several studies have shown that rotenone treatment can induce apoptosis in cells derived from human B cell lymphomas [5], promyelocytic leukemias [6], and neuroblastomas [7]. However, other studies contradict these findings; for example, one report suggests that rotenone actually inhibits bortezomib-induced ROS generation and cytochrome *c* release in human H460 non-small cell lung cancer cells [8].

Previous work demonstrated that supplementing rat diets with rotenone prevented cancers of the tongue induced by 4-nitroquinoline 1-oxide (4-NQO) [9]. Therefore, rotenone has potential as a novel candidate chemotherapeutic agent to treat oral cancer. Although studies have provided suggestive evidence for the therapeutic efficacy of rotenone in different cell types, the mechanism of action by which rotenone inhibits oral carcinogenesis is still unknown. Understanding the exact mode of action of rotenone should provide additional useful information toward its possible application in oral cancer treatment. In this report, we investigated the effects of rotenone on proliferation, the cell cycle, and apoptosis in human oral cancer cells. We also pursued a more detailed investigation of the mechanism of rotenone-induced cytotoxicity in oral cancer cells.

Materials and methods

Materials. All biological materials for tissue culture were obtained from Gibco Laboratories. Rotenone, glutathione (GSH), *N*-acetylcysteine (NAC), tiron, propidium iodide (PI), dimethyl sulfoxide (DMSO), 3-(4,5-dimethylthiazol-2-yl)-2, and 5-diphenyltetrazolium bromide (MTT) were obtained from Sigma Chemical Co. Protein determination kit was from BioRad Laboratories.

Cell culture. The SAS cell line was purchased from the Japanese Collection of Research Bioresources (Tokyo, Japan). The Cal27 cell line was from ATCC. The TW2.6 cell line was generated from a Taiwanese patient with buccal carcinoma [10]. The SAS cell line and oral mucosal fibroblasts (OMFs) were cultured in high-glucose Dulbecco's modified Eagle's medium, supplemented with 10% fetal calf serum

* Corresponding authors. Address: Genomics Research Center, Academia Sinica, 128, Academia Road, Section 2, Nankang District, Taipei 115, Taiwan. Fax: +886 2 27899931 (M. Hsiao). Address: Department of Dentistry, National Taiwan University Hospital, 1, Jen Ai Road, Section 1, Taipei 100, Taiwan. Fax: +886 2 23820785 (M.Y. Kuo).
E-mail addresses: mhsiao@gate.sinica.edu.tw (M. Hsiao), oddie@ccms.ntu.edu.tw (M.Y.P. Kuo).

0006-291X/$ - see front matter © 2008 Elsevier Inc. All rights reserved.
doi:10.1016/j.bbrc.2008.03.149

(FCS), 2 mM L-glutamine, penicillin (100 U/ml), and streptomycin (100 U/ml) at 37 °C in a humidified atmosphere of 95% air and 5% CO_2. For all experiments, cells were seeded in 35-mm Petri dishes at an initial density of 1×10^4 and allowed to attach for 24 h prior to rotenone treatment. The culture medium was replaced with fresh medium containing varying concentrations of rotenone and incubated for the indicated periods of time.

Cell viability (MTT) assay. Cell viability was measured using the MTT-based cytotoxicity assay, based on the ability of live cells to utilize tetrazolium and subsequently convert it into formazan. This assay detects living but not dead cells, and the signal directly correlates to the number of metabolically active cells in the culture. Briefly, cells were seeded in a 96-well plate and allowed to attach overnight. The cells were then treated with various concentrations of rotenone for 24, 48, and 72 h. On termination, MTT was added to each well at a final concentration of 0.5 mg/ml. After incubation for 4 h at 37 °C, medium and MTT were removed, and the MTT-formazan products were extracted with DMSO. The absorbance was read at 570 nm using a 96-well plate reader. Each data point is the average of results from eight wells.

Flow cytometric analysis. Tumor cells were harvested and stained with propidium iodide (PI) to determine intracellular DNA content by flow cytometry. This data was used to evaluate changes in the cell cycle following rotenone treatment, as previously described. Briefly, after seeding and overnight incubation, cells were treated with 1.25 μM rotenone. At the indicated time intervals, the cells were collected and fixed in ice-cold methanol/PBS (2:1 ratio) for a minimum of 30 min. Fixed cells were then stained in 0.5 ml of PBS containing 20 μg/ml DNase-free RNase A and 50 μg/ml PI for 30 min in the dark. The DNA content of the tumor cells was then determined by a Fluorescence Activated Cell Sorter (Becton Dickinson).

TdT-mediated dUTP nick end labeling (TUNEL) analysis. TUNEL staining was used to assay for apoptotic cells (Roche Applied Science). Cover slips were pre-treated with 1 N HCl and 95% ethanol and then seeded onto a 6-cm plate. Cells were treated as desired, followed by aspiration of the medium and the addition of fresh paraformaldehyde solution (4% in PBS, pH 7.4), which was used to fix cells for 30 min at room temperature. Cells were incubated with permeabilisation buffer (0.1% Triton® X-100, 0.1% sodium citrate) on ice. After washing cells twice with PBS, the TUNEL reaction mixture was added (composed of 5 μl enzyme solution mixed with 45 μl label solution, yielding 50 μl TUNEL reaction mixture for each sample). During staining, samples were incubated in the dark for 60 min at 37 °C prior to analysis. Cells were rinsed with PBS several times, followed by 30 s of PI staining (1 μg/ml) to counterstain the nucleus. After staining, the cover slip was inverted onto the slide, mounted with mounting solution, and sealed.

DNA ladder analysis. The formation of oligonucleosomal DNA fragments was examined by agarose gel electrophoresis. Briefly, 2×10^6 cells per 100-mm culture dish were treated with the indicated drugs. At different time points, both floating and adherent cells were harvested. After being washed once with PBS, cell pellets were subjected to genomic DNA purification using the Wizard® Genomic DNA Purification Kit (Promega), according to the manufacturer's instructions. Apoptotic oligonucleosomal DNA fragmentation was then assessed by gel electrophoresis (1.5% agarose).

Western blot analysis. Western blot analysis was used to assay for the apoptosis-related proteins expression, briefly, cells in 10-cm plates were harvested at the indicated time points and washed with PBS. Cells were lysed in 100 μl lysis buffer (20 mM Tris–HCl, pH 7.4, 150 mM NaCl, 0.5% Nonidet P-40, 1 mM EDTA, 50 μg/ml leupeptin, 30 μg/ml aprotinin, and 1 mM PMSF) and subjected to 12.5% PAGE. A total volume of 30 μg of protein was loaded per lane. The separated proteins were blotted onto a nitrocellulose membrane (PALL Gelman Laboratory) by semi-dry transfer (BIO-RAD). After blocking with 5% milk in TBST, the membranes were then incubated with various antibodies: p53, Bcl-2, Bcl-$X_{S/L}$, caspase-3 (Santa Cruz Biotechnology), p21, Bax (BD Transduction Laboratory), caspase-8, caspase-9, cleaved caspase-3, PARP (Cell Signaling), cytochrome *c* (BD PharMingen), or β-actin (Sigma). The following dilutions were used: p53 1:1000, Bcl-2 1:500, Bcl-$X_{S/L}$ 1:1000, p21 1:500, Bax 1:250, caspase-8 1:1000, caspase-9 1:1000, cleaved caspase-3 1:500, PARP 1:1000, caspase-3 1:1000, cytochrome *c* 1:1000, and β-actin 1:10000. After primary antibody incubation, the membranes were incubated with HRP-labeled secondary antibody (Promega) at a concentration of 1:10,000. The Western Lighting Chemiluminescence Reagent (Perkin Elmer) was then added and then exposed with Fuji X-ray film. The results were digitized for densitometric analysis using the Gel Pro Analyzer.

Apoptosis ELISA analysis with caspase and ROS inhibitors. Cells were seeded onto 48-well microtiter plates at 5×10^4/well, grown for 24 h, and pre-treated for 3 h with 100 mM of the caspase-8 inhibitor, Z-IETD-FMK, or the caspase-9 inhibitor, Z-LEHD-FMK (Calbiochem). For ROS inhibitor experiments, cells were treated with 15 mM glutathione, 15 mM *N*-acetylcysteine, or 1 mM tiron for 30 min. Afterwards, 1 μM of rotenone was added for 24 h. Apoptosis was analysis by the Cell Death Detection ELISA assay (Roche Applied Science). Briefly, cell lysates were pipetted onto a streptavidin-coated 96-well microtiter plate to which the immunoreagent mix was added and incubated for 2 h at room temperature. The wells were then washed, treated with substrate solution, and developed for 10–20 min. Absorbance was read at 405 nm against the blank at a reference wavelength of 490 nm. The enrichment factor (amount of apoptosis) was calculated by dividing the absorbance of the sample (405 nm) by the absorbance of the untreated controls (490 nm).

Statistical analysis. Group data are expressed as means ± SD. The unpaired Student's *t* test (for control and study group comparisons) was applied to compare group differences. Differences with $P < 0.05$ were considered significant.

Results

Cell growth inhibition caused by rotenone

The effects of various concentrations of rotenone (0–60 μM) were examined by MTT assay in both oral cancer cell lines (SAS, Cal27, and Tw2.6) and normal oral mucosal fibroblasts (OMFs). The results showed rotenone significantly inhibited the proliferation of all three oral cancer cell lines compared to oral mucosal fibroblasts in a concentration-dependent manner (Fig. 1A). The 50% inhibitory concentrations (IC_{50}) after 48 h of rotenone treatment for SAS, Cal27, Tw2.6, and OMFs were 0.95 ± 0.05, 0.11 ± 0.02, 1.24 ± 0.11, and 31.43 ± 2.31 μM, respectively; the selective indices for OMF/SAS, OMF/Cal27, and OMF/Tw2.6 were 33.08, 28.57, and 25.34, respectively.

Induction of apoptosis by rotenone treatment

To examine the effect of rotenone on cell cycle progression, SAS cells were treated with 1 μM rotenone for 0, 12, 24, 48, and 72 h. The cell cycle phase distribution was then analyzed by flow cytometry. As shown in Fig. 1B, treatment with rotenone resulted in the accumulation of cells in G_2/M phase. The G_2/M blockade peaked at 12 h, with approximately 70% of cells in G_2/M at that time point, compared to 25–30% in controls (Table 1). At later time points, the number of sub-G_1 cells (apoptotic cells) gradually increased. The percentage of accumulated sub-G_1 apoptotic cells was approximately 52% after 72 h of exposure to rotenone. Similar results were also found in Cal27 and Tw2.6, which showed a smaller proportion of sub-G_1 cells. The OMFs did not show any significant cell cycle profile changes at 72 h after 1 μM rotenone treatment (data not shown).

To further investigate whether rotenone-induced growth inhibition in this cell line was caused by apoptosis, TUNEL (TdT-mediated dUTP nick end labeling) analysis of apoptotic DNA fragments was performed. Cells positive for TUNEL staining were found to have condensed and/or fragmented nuclei (Fig. 1C). Approximately 40% of the cells were apoptotic by 48 h after rotenone treatment. Similar results were also observed from analysis of DNA fragmentation by gel electrophoresis. As shown in Fig. 1D, DNA cleavage into oligonucleosomal fragments (180–200 base pairs), a typical feature of apoptosis, was observed in SAS cells after 24–72 h of rotenone exposure (Fig. 1E).

Rotenone induces cytochrome c release and caspase activation

To investigate the mechanisms of rotenone-induced apoptosis in oral cancer cell lines, we next investigated the levels of cytochrome *c* in the soluble cytosolic fraction of SAS cells after rotenone treatment. Treatment of SAS cells with 1 μM rotenone caused cytochrome *c* release into the cytosol (Fig. 2A), where the amount of cytochrome *c* released into the cytosol increased in a time-dependent manner. Furthermore, we examined the cleavage of procaspase-8 and procaspase-9 in cells following rotenone treatment. Immunoblotting analysis demonstrated that both caspases were cleaved into their characteristic active fragments after SAS cells were treated with 1 μM rotenone. At 24 h, active caspase-8 increased 8-fold in SAS cells, while the cleaved form of caspase-9 increased 3-fold (Fig. 2B).

The involvements of caspase-9 and caspase-8 in rotenone-induced apoptosis were further validated by using caspase inhibitors. As shown in Fig. 3A and B, rotenone-induced apoptosis was again

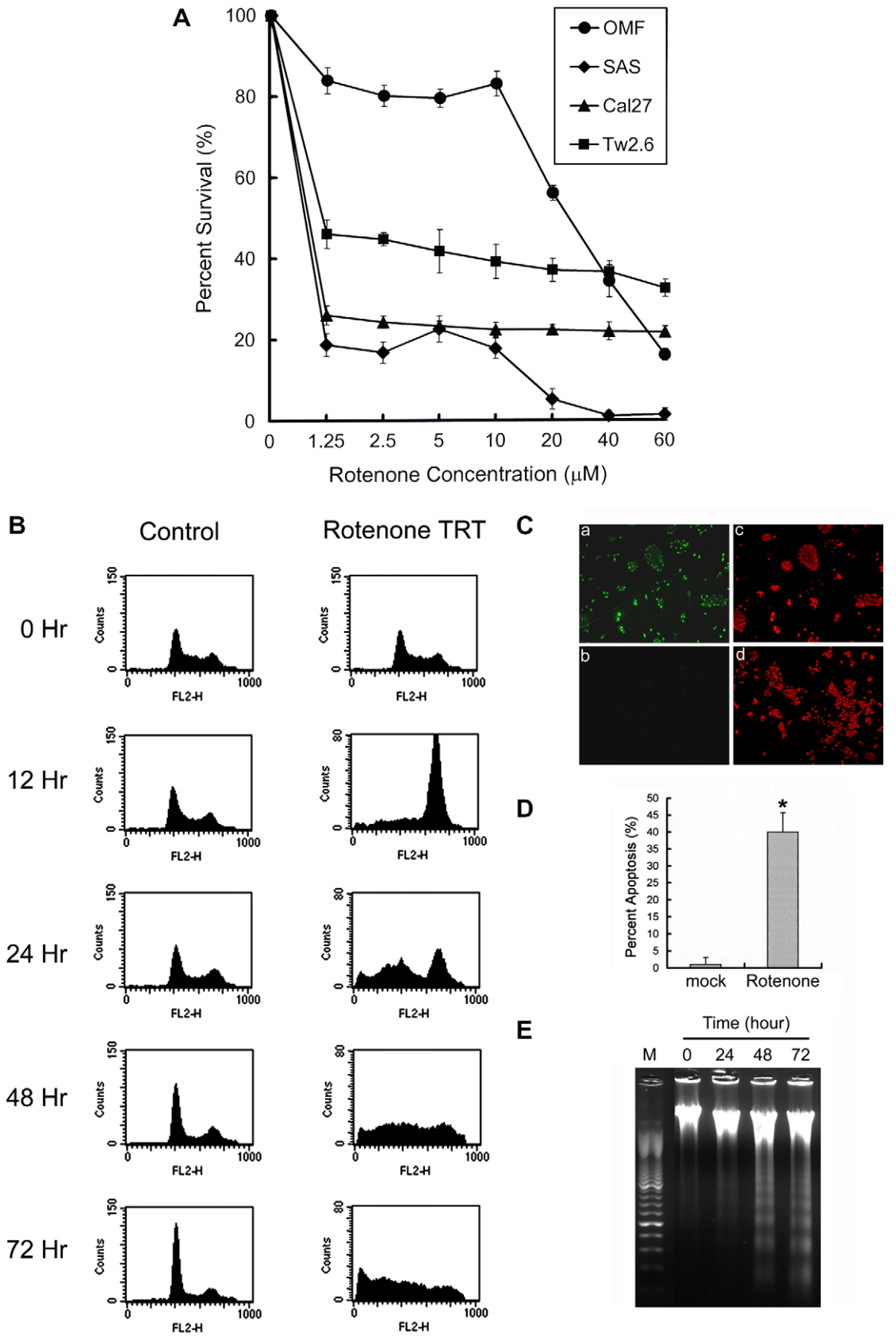

Fig. 1. Effects of rotenone on the cytotoxicity of oral cancer cell lines and oral mucosal fibroblasts (OMFs). (A) Cells were treated with increasing concentrations of rotenone (0–60 μM) for 72 h. Viable cells were measured by MTT assay and expressed as a percentage of control (n = 8). All values are means of three independent experiments ± SEM (bars). (B) Cell cycle phase distribution of SAS cells treated with 1 μM rotenone for the indicated times, analyzed by flow cytometry. (C) TUNEL staining analysis of rotenone-treated SAS cells treated with 1 μM rotenone for 48 h and visualized by fluorescence microscopy after staining with PI (c) or TUNEL (a, upper panel). Note the apoptotic cells with nuclear condensation, fragmentation, and positive TUNEL signal compared to control cells (b and d). Magnification, 100×. (D) Percentage of cells undergoing apoptosis observed by TUNEL staining. Results are the means of three independent experiments. (E) DNA ladder analysis of SAS cells treated with rotenone.

Table 1
Percent cell cycle distributions after rotenone treatment in SAS cells

	0 h	12 h	24 h	48 h	72 h
Sub-G1	1.4 ± 0.1%[a]	12.1 ± 1.9%	32.0 ± 2.2%	38.9 ± 2.4%	52.1 ± 1.7%
G1	46.2 ± 2.5%	7.4 ± 0.9%	15.1 ± 0.6%	17.7 ± 0.9%	16.3 ± 1.4%
S	19.5 ± 0.8%	10.5 ± 1.2%	12.3 ± 1.1%	15.2 ± 1.3%	12.1 ± 0.8%
G2/M	32.9 ± 1.8%	70.0 ± 3.2%	40.6 ± 5.3%	28.2 ± 2.2%	19.5 ± 1.6%

[a] Percentage of cells in each cell cycle compartment were determined by deconvolution of the DNA content-frequency histogram. The tabulated percentages are an average calculated on the results of three separate experiments.

determined by quantitating cytoplasmic histone-associated DNA fragments. Apoptosis was significantly attenuated after treating cells with specific inhibitors of caspase-8 (Z-IETD-FMK) and caspase-9 (Z-LEHD-FMK). Co-treatment with both caspase-8 and caspase-9 inhibitors further reduced the number of cells undergoing apoptosis.

Inhibition of rotenone-induced apoptosis by antioxidants

To test whether ROS plays a role in rotenone-induced apoptosis in SAS cells, we used three antioxidants—glutathione, NAC, and tiron—to evaluate their effects on rotenone-induced apoptosis. As shown in Fig. 3C, all three antioxidants decreased rotenone-induced apoptosis. Among these antioxidants, tiron was shown to be the most potent.

Rotenone increases the expression of p53 and Bax protein

The cytochrome *c*-initiated caspase cascade has been shown to be regulated by the Bcl-2 family of proteins. The balance between anti-apoptotic and pro-apoptotic Bcl-2 family members is critical in determining the susceptibility of cells to death. Therefore, the influence of rotenone on proteins of this family was examined. Rotenone induced the upregulation of Bax by 12 h (3-fold) and the maintenance of Bax expression levels for an additional 48 h (2-fold). No change in the expression levels of Bcl-$X_{S/L}$ and Bcl-2 was induced by rotenone in SAS cells (Fig. 4). The Bax gene is a known downstream target of p53, which transactivates Bax. We also found that rotenone enhanced the expression of p53 from 12 to 48 h in SAS cells. However, the expression of another p53 downstream target, p21, was not increased following treatment with rotenone.

Discussion

In the present study, rotenone treatment caused significant apoptosis in SAS cells, as demonstrated by flow cytometric detection of sub-G_1 DNA content, TUNEL labeling, DNA fragmentation, caspase-3 activation, and PARP cleavage. Shimizu et al. suggested that rotenone and other inhibitors of mitochondrial electron transport do not cause apoptosis, but induce necrotic cell death [11]. However, others have shown that cells treated with rotenone undergo apoptosis [12]. The ability of rotenone to induce apoptosis or necrosis may depend upon the cell type studied, since cellular demise by apoptotic mechanisms occurs readily in many cell types, but in other cells is more difficult to induce [13].

The differential toxicity of rotenone in oral cancer cells and OMFs may be due to the fact that cancer cells are under increased oxidative stress compared to normal OMFs. Normal cells are protected by antioxidant enzymes (e.g., catalase, superoxide dismutase, and glutathione peroxidase) from the toxic effects of high concentrations of ROS generated during cellular metabolism. However, these antioxidant enzyme levels are low in most animal and

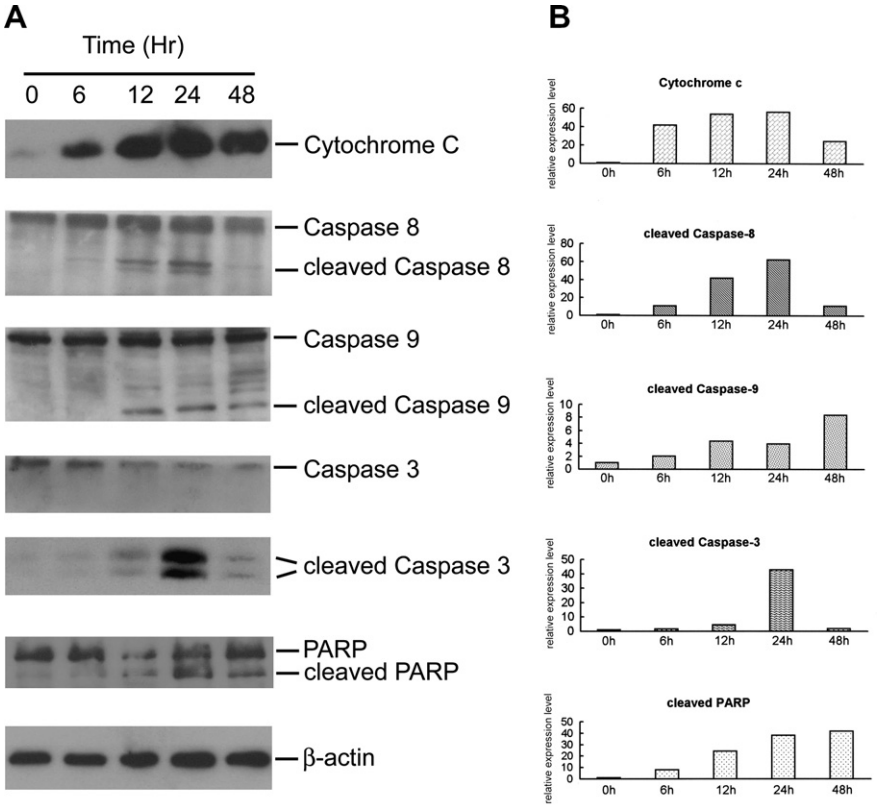

Fig. 2. Western blot analysis of apoptosis-related gene expression after rotenone treatment. (A) Note cytochrome *c* following rotenone treatment. The active forms of caspase-8 (43 kDa) and caspase-9 (35 and 37 kDa) were detected after a 12 h exposure to rotenone. Cleaved caspase-3 (17 and 19 kDa) and the 85 kDa-cleavage product of PARP increased with time. β-Actin was used as an internal control. (B) Kinetics of apoptosis-related gene expression. Densitometry units represent the expression level of the target protein divided by the expression level of β-actin.

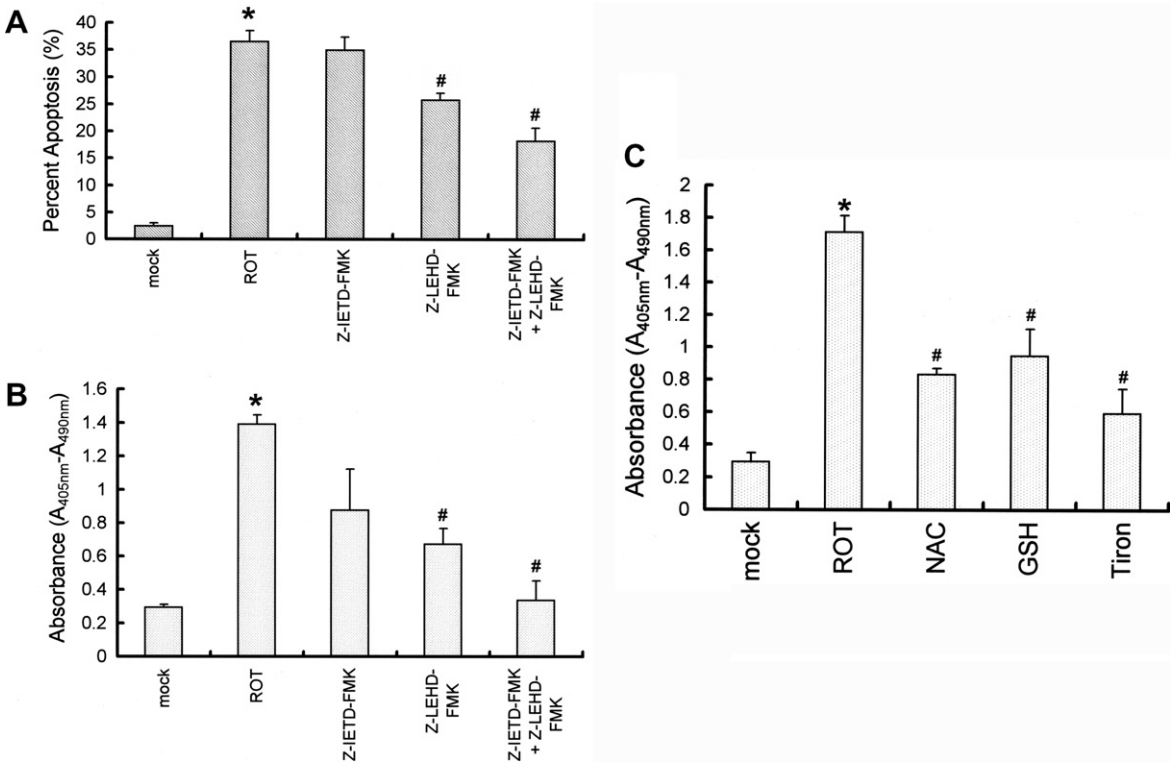

Fig. 3. Inhibition of rotenone-induced apoptosis in SAS cells by caspase or ROS inhibitors. (A) Caspase inhibitor effects measured by the percentage of cells at sub-G1 phase by flow cytometry. (B) Cell death detection ELISA. Data are expressed as means ± SEM ($n = 4$, $^{*}P < 0.01$ compared to mock, $^{\#}P < 0.05$ compared to rotenone treatment). (C) ROS inhibitor effects measured by cell death detection ELISA. Data were expressed as means ± SEM ($n = 4$, $^{*}P < 0.01$ compared to mock, $^{\#}P < 0.05$ compared to rotenone treatment).

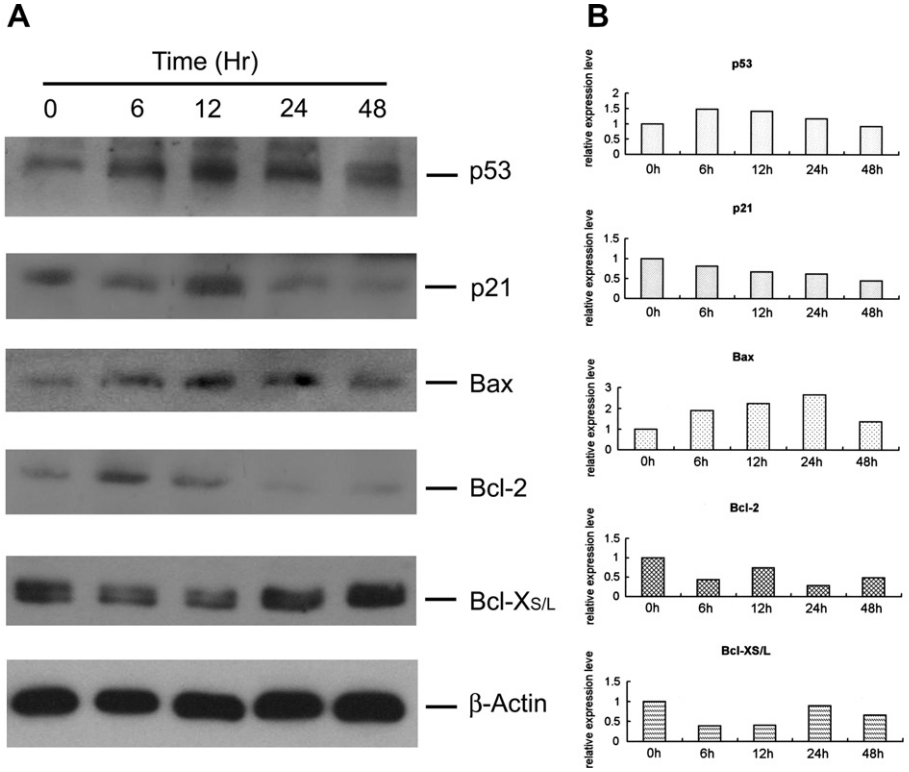

Fig. 4. Western blot analysis of p53 and p53-related downstream gene expression in SAS cells following rotenone treatment. (A) SAS cells were cultured in the presence of 1 μM rotenone for the indicated time intervals. Note that p53 and Bax expression increased over time after rotenone treatment, while other genes did not change significantly. β-Actin was used as an internal control. (B) Kinetics of p53 and p53-related downstream gene expression in SAS cells after rotenone treatment. Densitometry units represent the expression level of the target protein divided by the expression level of β-actin.

human cancers [14], and the concentrations of free oxygen radicals are higher in malignant cells than their normal counterparts [15]. Therefore, cancer cells are more vulnerable to additional oxidative stress caused by exogenous ROS-generating agents. This hypothesis is supported by the observations that ROS appear to be an important mediator of the activity of rotenone. Furthermore, rotenone may be useful in combination with other ROS-generating agents, such as doxorubicin, bleomycin, and cisplatin, to enhance their anticancer activity.

Since many anticancer drugs kill tumor cells by inducing apoptosis, this cell death pathway represents an important mechanism to exploit. It is known that rotenone induces apoptosis in cells derived from human B cell lymphomas and neuroblastomas, but the mechanisms involved are different for each case. Armstrong et al. showed that rotenone induced G_2/M cell cycle arrest and apoptosis in a human B cell lymphoma cell line, PW [5]. During apoptosis, the activation of caspases leads to the cleavage and inactivation of key cellular proteins, such as PARP. Caspase-3 is an "executioner caspase" that can be activated by a mitochondrial pathway involving caspase-9, or a death receptor pathway involving caspase-8. Treating PW cells with rotenone led to the biochemical features of apoptosis, including mitochondrial cytochrome *c* release, ROS generation, and the activation of procaspase-3. The inhibition of mitochondrial electron transport by rotenone may be insufficient to induce apoptosis in PW cells. Instead, apoptosis in these cells may occur as a consequence of disrupting the cell cycle, and is only indirectly dependent upon mitochondrial electron transport. In neuroblastoma cells, rotenone induces activation of both mitochondria- and endoplasmic reticulum-dependent caspases [7]. In leukemic cells, partial inhibition of mitochondrial respiration by rotenone enhances electron leakage from the transport chain, leading to an increase in the generation of superoxide radicals and sensitization of the leukemia cells to anticancer agents whose action involves free radical generation [6]. However, rotenone inhibits bortezomib-induced ROS generation and cytochrome *c* release in human H460 non-small cell lung cancer cells [8]. In our model, PARP cleavage was observed within 12 h of rotenone treatment. Rotenone treatment also caused cleavage of both procaspase-9 and procaspase-8. Moreover, rotenone-induced apoptosis was significantly attenuated in the presence of specific inhibitors of caspase-8 and caspase-9 (Fig. 3). These results suggest the involvement of both mitochondrial and death receptor pathways in rotenone-induced apoptosis of oral cancer cells. Further characterization of the mitochondrial and death receptor pathways in rotenone-treated cells would help establish the relative contributions of the caspase-9 and caspase-8 cascades to rotenone-induced apoptosis. The role of ROS in rotenone-induced apoptosis of oral cancer cells also needs to be elucidated.

The G_2/M cell cycle arrest observed after rotenone treatment may be a direct consequence of inhibiting the polymerization of microtubules, since Barrietos et al. and other groups have shown this effect with rotenone. Indeed, inhibiting microtubule polymerization is known to affect the ability of cells to enter and exit the cell cycle during mitosis [16–18]. Inhibiting caspase activation with specific inhibitors of caspase-8 and caspase-9 blocked apoptosis, but did not prevent G_2/M arrest, indicating that apoptosis occurs downstream of cell cycle arrest. The tumor suppressor protein, p53, has previously been suggested to play a role in G_2/M arrest as well as G1 arrest [19].

In conclusion, our results showed that rotenone is more effective in inducing cytotoxicity in oral cancer cells than in normal OMFs. This growth inhibition was due to G_2/M cell cycle arrest, which led to apoptosis via the activation of both the caspase-8 and caspase-9 pathways. ROS were found to be important mediators of rotenone-induced apoptosis. Furthermore, p53 and Bax may play important roles in rotenone-induced apoptosis upstream of caspase activation by upregulating and/or preventing the degradation of apoptosis-related proteins.

Acknowledgment

This work was supported in part by grants from the National Science Council (to M.H. and M.Y.K.); and Academia Sinica (to M.H.).

References

[1] T.B. Sherer, R. Betarbet, A.K. Stout, S. Lund, M. Baptista, A.V. Panov, M.R. Cookson, J.T. Greenamyre, An in vitro model of Parkinson's disease: linking mitochondrial impairment to altered alpha-synuclein metabolism and oxidative damage, J. Neurosci. 22 (2002) 7006–7015.
[2] T.B. Sherer, J.H. Kim, R. Betarbet, J.T. Greenamyre, Subcutaneous rotenone exposure causes highly selective dopaminergic degeneration and alpha-synuclein aggregation, Exp. Neurol. 179 (2003) 9–16.
[3] Y. Ren, J. Feng, Rotenone selectively kills serotonergic neurons through a microtubule-dependent mechanism, J. Neurochem. 103 (2007) 303–311.
[4] N. Li, K. Ragheb, G. Lawler, J. Sturgis, B. Rajwa, J.A. Melendez, J.P. Robinson, Mitochndrial complex I inhibitor rotenone induces apoptosis through enhancing mitochondrial reactive oxygen species production, J. Biol. Chem. 278 (2002) 8516–8525.
[5] J.S. Armstrong, B. Hornung, P. Lecane, D.P. Jones, S.J. Knox, Rotenone-induced G2/M cell cycle arrest and apoptosis in a human B lymphoma cell line PW, Biochem. Biophys. Res. Commun. 289 (2001) 973–978.
[6] S. Tada-Oikawa, Y. Hiraku, M. Kawanishi, S. Kawanishi, Mechanisms of generation of hydrogen peroxide and change of mitochondrial membrane potential during rotenone-induced apoptosis, Life Sci. 73 (2003) 3277–3288.
[7] W.G. Chung, C.L. Miranda, C.S. Maier, Epigallocatechin gallate (EGCG) potentiates the cytotoxicity of rotenone in neuroblastoma SH-SY5Y cells, Brain Res. 1176 (2007) 133–142.
[8] Y.H. Ling, L. Liebes, Y. Zou, R. Perez-Soler, Reactive oxygen species generation and mitochondrial dysfunction in the apoptotic response to Bortezomib, a novel proteasome inhibitor, in human H460 non-small cell lung cancer cells, J. Biol. Chem. 278 (2003) 33714–33723.
[9] T. Tanaka, H. Kohno, K. Sakata, Y. Yamada, Y. Hirose, S. Sugie, H. Mori, Modifying effects of dietary capsaicin and rotenone on 4-nitroquinoline 1-oxide-induced rat tongue carcinogenesis, Carcinogenesis 23 (2002) 1361–1367.
[10] S.H. Kuo, C.Y. Hong, S.K. Lin, J.J. Lee, C.P. Chiang, M.Y. Kuo, Establishment and characterization of a tumorgenic cell line from areca quid and tobacco smake-associated buccal carcinoma, Oral Oncol. 43 (2007) 639–647.
[11] S. Shimizu, Y. Eguchi, W. Kamiike, S. Waguri, Y. Uchiyama, H. Matsuda, Y. Tsujimoto, Retardation of chemical hypoxia-induced necrotic cell death by Bcl-2 and ICE inhibitors: possible involvement of common mediators in apoptotic and necrotic signal transductions, Oncogene 12 (1996) 2045–2050.
[12] K. Yuki, T. Miyauchi, Y. Kakinuma, N. Murakoshi, T. Suzuki, J. Hayashi, K. Goto, I. Yamaguchi, Mitochondrial dysfunction increases expression of endothelin-1 and induces apoptosis through caspase-3 activation in rat cardiomyocytes in vitro, J. Cardiovasc. Pharmacol. 36 (2000) S205–S208.
[13] J. Kovar, T. Valenta, H. Stybrova, Differing sensitivity of tumor cells to apoptosis induced by iron deprivation in vitro, In Vitro Cell. Dev. Biol. Anim. 37 (2001) 450–458.
[14] T.D. Oberley, L.W. Oberley, Antioxidant enzyme levels in cancer, Histol. Histopathol. 12 (1997) 525–535.
[15] S. Toyokuni, K. Okamoto, J. Yodoi, H. Hiai, Hypothesis: persistent oxidative stress in cancer, FEBS Lett. 358 (1995) 1–3.
[16] A. Barrientos, C.T. Moraes, Titrating the effects of mitochondrial complex I impairment in the cell physiology, J. Biol. Chem. 274 (1999) 16188–16197.
[17] L.E. Marshall, R.H. Himes, Rotenone inhibition of tubulin self-assembly, Biochim. Biophys. Acta 543 (1978) 590–594.
[18] B.R. Brinkley, S.S. Barham, S.C. Barranco, G.M. Fuller, Rotenone inhibition of spindle microtubule assembly in mammalian cells, Exp. Cell Res. 85 (1974) 41–46.
[19] W.R. Taylor, G.R. Stark, Regulation of the G2/M transition by p53, Oncogene 20 (2001) 1803–1815.